



ELSEVIER

Polymer 44 (2003) 2187–2191

polymerwww.elsevier.com/locate/polymer

Polymer Communication

Thermal properties and hydrogen bonding in polymer blend of polybenzoxazine/poly(*N*-vinyl-2-pyrrolidone)

Yi-Che Su^a, Shiao-Wei Kuo^a, Ding-Ru Yei^a, Hongyao Xu^{a,b}, Feng-Chih Chang^{a,*}^a*Institute of Applied Chemistry, National Chiao-Tung University, Hsin-Chu, Taiwan, ROC*^b*Department of Chemistry, Anhui University, Anhui 230039, People's Republic of China*

Received 29 July 2002; received in revised form 14 November 2002; accepted 16 December 2002

Abstract

The thermal properties and hydrogen bonding behavior of B-a type polybenzoxazine (PBZZ)/PVP blends were investigated by DSC and FTIR. The DSC result shows a single T_g over the entire compositions and a large positive deviation based on Kwei equation was observed in the T_g versus composition diagram, implying that strong hydrogen bonding interaction exists between PBZZ and PVP segments. The strength of hydrogen bonding interaction is in the order of inter-association between the hydroxyl group of PBZZ and the carbonyl group of PVP ($K_A = 594 \text{ L mol}^{-1}$) > self-association between the hydroxyl group of pure PBZZ ($K_B = 72.6 \text{ L mol}^{-1}$) > inter-association between the hydroxyl and the Mannich-based bridge of pure PBZZ ($K_C < 10 \text{ L mol}^{-1}$). Good correlation between DSC and FTIR analysis were observed.

© 2003 Elsevier Science Ltd. All rights reserved.

Keywords: Hydrogen bonding; Polybenzoxazine; Polymer blend

1. Introduction

The structure of PBZZ is similar to phenolic resin through thermal self-curing of the heterocyclic ring opening reaction that neither requires catalyst nor releases any condensation byproduct [1]. These PBZZ resins were found to possess several outstanding properties such as near-zero shrinkage after curing, high thermal stability and low water absorption [2]. Furthermore, the PBZZ has high glass transition temperatures even though it has relatively low crosslinking density [3].

The PBZZ possess the hydroxyl group that is expected to form intermolecular hydrogen bonding with other polymers with a proton-accepter. Since PVP [4,5] is a water-soluble tertiary amide and a Lewis base that possesses good biocompatibility. The PVP contains carbonyl group that is known as a strong proton acceptor for several polymers with proton donor [6,7].

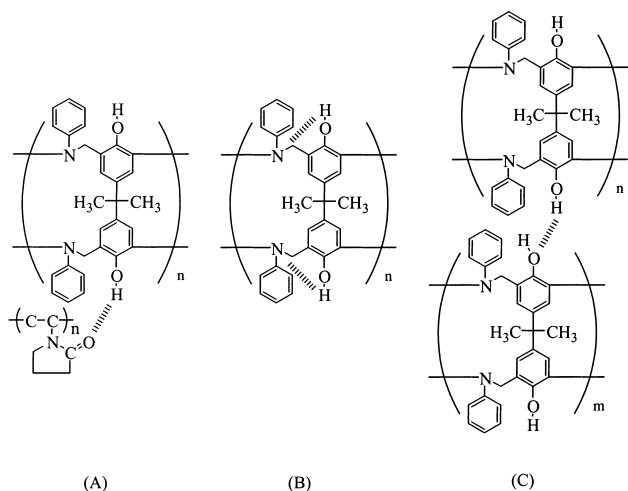
In order to better understand the hydrogen bonding interaction of the pure PBZZ and the PBZZ/PVP blend systems, a series of model compounds are used to simulate the miscibility behavior of analogous hydrogen bonded

polymer blends [8,9]. In this blend system, these equilibria can be described by four different constants: two self-association equilibrium constants describing the formation of hydrogen bonded dimer (K_2) and multimers (K_B) of the PBZZ hydroxyls, inter-association equilibrium constants (K_A and K_C) between PBZZ hydroxyl and PVP carbonyl, and the inter-molecular interaction between hydroxyl and Mannich-based bridge both of pure PBZZ, respectively. Blend of 4-isopropylphenol (IPP)/1-ethyl-2-pyrrolidinone (EPr) has been employed to simulate the PBZZ/PVP blend. In addition, an extra inter-association hydrogen bonding can be attributed to the hydroxyl group of IPP and the Mannich based bridge ($-\text{CH}_2-\text{NAr}-\text{CH}_2$) (which replaced by using *N,N*-dimethylaniline (DMA)) both of pure PBZZ. The self- and inter-association hydrogen bonding interactions of this blend system can be represented by Scheme 1.

2. Experimental

Benzoxazine (B-a type) was synthesized ourselves. Poly(*N*-vinyl-2-pyrrolidone) (PVP) used in this study was purchased from Aldrich of USA with the $M_w = 58,000$. 4-isopropyl Phenol (IPP), 1-ethyl-2-pyrrolidone (EPr), and

* Corresponding author. Tel.: +886-3-5727077; fax: +886-3-5723764.
E-mail address: changfc@cc.nctu.edu.tw (F.C. Chang).



Scheme 1. The schematic representation of hydrogen bonding (A) inter-association of PBZZ/PVP blend, (B) intra-association of the pure PBZZ, (C) inter-association of the pure PBZZ.

N,N-dimethylaniline (DMA) were purchased from Acros Chemical Company of USA. Blends of benzoxazine/PVP with several different compositions were prepared by solution blending. Afterwards, it was cured at 180 °C for 4 h under vacuum to ensure total curing of the benzoxazine. A DSC from Du-Pont (DSC-2010) was used to measure T_g s of these blends. The sample was preheated with a scan rate of 20 °C min⁻¹ from 30 to 260 °C for the first scan and maintained at 260 °C for 2 min. The DSC sample was cooled to 100 °C (below each polymer blend's T_g) slowly

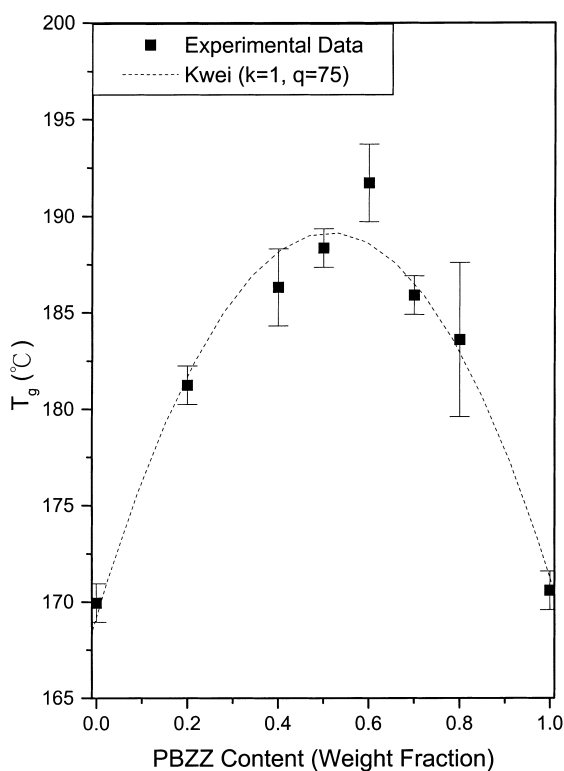


Fig. 1. T_g versus composition curve based on PBZZ/PVP blends.

and then quickly cooled to 30 °C. The second scan rate was 20 °C min⁻¹ from 30 to 300 °C. FT-IR measurement was recorded on a Nicolet Avatar 320 FT-IR spectrophotometer, 32 scans were collected with a spectral resolution of 1 cm⁻¹. Infrared spectra of the polymer blends were obtained using the conventional NaCl disk method. For the sample in solution form, a sealed cell with NaCl windows and 0.2 mm sample thickness was used. Cyclohexane (CHEX) was selected as the solvent because it is low polar and does not form any interaction with model compounds used in the study.

3. Results and discussion

3.1. Glass transition temperature analysis

Fig. 1 shows the dependence of the T_g on the composition of PBZZ/PVP blends. A single T_g implies that blends of PBZZ and PVP are miscible in the amorphous phase. In addition, the maximum T_g deviation is obtained when blend composition at PBZZ/PVP = 60/40 (weight ratio). Kwei equation [10] describes the effect of T_g hydrogen bonding interaction between polymers as shown in Eq. (1):

$$T_g = \frac{W_1 T_{g1} + kW_2 T_{g2}}{(W_1 + kW_2)} + qW_1 W_2 \quad (1)$$

where W_1 and W_2 are weight fractions of the components, T_{g1} and T_{g2} represent the component's glass transition

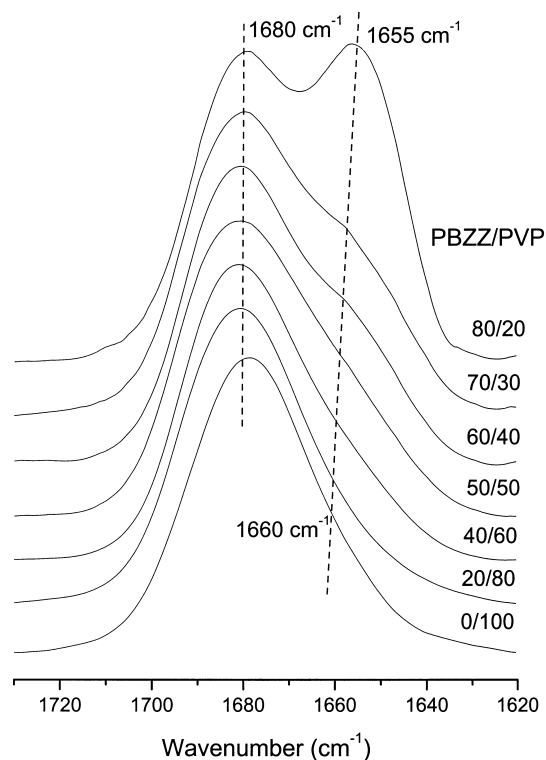


Fig. 2. FTIR spectra recorded at room temperature between 1620 and 1730 cm⁻¹.

temperatures. Both k and q are fitting constants. In general, the parameter q may be considered as a measurement of the specific interaction in a polymer blend system. When the intermolecular interaction is stronger than intramolecular interaction in a binary blend, the value of q will be positive; otherwise, q will be negative. When the q value is larger, it represents that the interaction is stronger than the self-interaction of the blend.

After the ‘best fitting’ by the Kwei equation, $k = 1$ and $q = 75$ were obtained. In this study, a large positive q value of 75 indicates that a strong intermolecular interaction exists between PBZZ and PVP.

3.2. Fourier transfer infrared spectroscopy analysis

Fig. 2 shows the infrared spectra of the carbonyl stretching of various PBZZ/PVP blends. The pure PVP gives a broad carbonyl absorption peak at 1680 cm^{-1} [11, 12]. After adding the PBZZ into the PVP system, the carbonyl stretching frequency is split into two bands at 1680 and 1660 cm^{-1} , corresponding to the free and the hydrogen-bonded carbonyl groups, respectively. This free carbonyl band (1680 cm^{-1}) gradually shifts into the hydrogen-bonded carbonyl (1655 cm^{-1}) with increasing of the PBZZ content in the blend. These two carbonyl bands can be fitted well to the Gaussian function and the fraction of the hydrogen-bonded carbonyl group can be calculated according to Eq. (2) [13] and summarizes in Table 1.

$$f_b^{C=O} = \frac{A_b/1.3}{A_b/1.3 + A_f} \quad (2)$$

A_f and A_b denote peak areas corresponding to the free and the hydrogen-bonded carbonyl groups. The absorptions, ratio $\varepsilon_2/\varepsilon_1 = 1.3$, was taken from previous infrared studies in hydroxyl–carbonyl inter-association [14].

3.3. The self-association of hydroxyl groups of PBZZ

According to the Painter–Coleman Association Model [8], we designate 2, B, C, and A as dimers of PBZZ, multimers of PBZZ, Mannich based bridge and PVP units,

Table 1
Curve fitting of fraction of hydrogen-bonding results of the PBZZ/PVP blends at room temperature

PBZZ /PVP	Free C=O		H-bonded C=O		f_b (%)
	ν (cm^{-1})	A_f (%)	ν (cm^{-1})	A_b (%)	
80/20	1680.1	56.62	1654.6	43.38	37.08
70/30	1682.2	63.98	1657.5	36.02	30.22
60/40	1682.5	64.98	1658.5	35.02	29.31
50/50	1685.2	68.15	1665.4	31.85	26.45
40/60	1684.2	77.84	1666.0	22.16	17.96
20/80	1682.4	85.71	1662.8	14.29	11.36

f_b = fraction of hydrogen bonding.

respectively, and K_2 , K_B , K_C and K_A as their corresponding association equilibrium constants.

In this study, we choose the 4-isopropylphenol (IPP) to replace the PBZZ unit because the pure PBZZ is not soluble in CHEX. In addition, the CHEX does not exhibit fundamental vibrational frequencies in the hydroxyl ($3100\text{--}3700\text{ cm}^{-1}$) or carbonyl ($1600\text{--}1800\text{ cm}^{-1}$) stretching regions of the infrared spectrum. The self-association of hydroxyl groups can be analyzed from the infrared spectra of IPP/CHEX mixtures by increasing from 0.00125 to 0.5 M . These overtone and combination bands were eliminated by spectral subtraction in the spectra of the more dilute solutions. By increasing the concentration of IPP above 0.01 M , the effect of self-interaction of dimers and multimer becomes noticeable; especially the multimers one as shown in Fig. 3(a). In order to calculate the self-association equilibrium constant [1,15], we need to measure the fraction of free monomers in the dilute solution of a given concentration of IPP. The intensity (absorbance) of the isolated hydroxyl band (at 3620 cm^{-1}), I , is related to absorptivity coefficient, ε , the concentration c , and the path length l , using the Beer-Lambert law, $I = c.\varepsilon.l$. The value of absorptivity coefficient (ε) is determined by plotting (I/c) versus c , the value of ε of 31.1 is obtained through Eq. (3)

$$\lim_{c \rightarrow 0} \left| \frac{I}{cl} \right| = \varepsilon \quad (3)$$

The experimental fraction of free monomer, f_m^{OH} and the value of $\varepsilon (= I/cl)$, at any given concentration of IPP was calculated by Eq. (4) and summarized in Table 2. When the concentration of the IPP is increased; the fraction of free hydroxyl group is decreased gradually.

$$f_m^{\text{OH}} = \frac{I}{I_0} \quad (4)$$

There are two equilibrium constants that can describe the

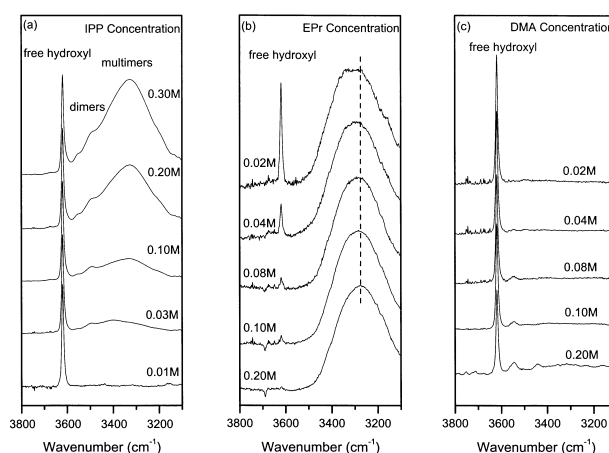
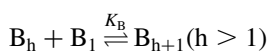


Fig. 3. (a) Infrared difference spectra of IPP/CHEX solutions with different IPP concentrations recorded at room temperature. (b) Infrared difference spectra of IPP (0.02 M)/EPr/CHEX solutions recorded at room temperature. (c) Infrared difference spectra of IPP (0.02 M)/DMA/CHEX solutions recorded at room temperature.

Table 2
IPP/CHEX data

C_{IPP} (M)	l/cl	f_m^{OH}	C_{IPP} (M)	l/cl	f_m^{OH}
0.00125	30.6	0.983	0.08	17.63	0.566
0.0025	30.34	0.975	0.1	15.9	0.511
0.005	29.9	0.961	0.2	10.0	0.321
0.001	29.1	0.935	0.3	7.48	0.240
0.02	27.0	0.867	0.4	6.11	0.196
0.04	23.0	0.739	0.5	4.92	0.158
0.06	19.75	0.635			

self-association of IPP containing hydroxyl groups, the formation of dimers (K_2) and the formation of multimers complex (K_B) as shown in Eq. (5)



where B_1 , B_2 and B_h represent the hydroxyl group, hydroxyl/hydroxyl dimers and hydroxyl/hydroxyl multimers of PBZZ, respectively.

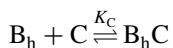
Finally, we used Eq. (6) [8] to obtain the best fit of K_2 and K_B for IPP, $K_2 = 28.3 \text{ L mol}^{-1}$ and $K_B = 72.6 \text{ L mol}^{-1}$ were obtained then.

$$f_m^{\text{OH}} = \frac{\Phi_{B1}}{\Phi_B} = \left[\left(1 - \frac{K_2}{K_B} \right) + \frac{K_2}{K_B} \left(\frac{1}{(1 - K_B \Phi_{B1})^2} \right) \right]^{-1} \quad (6)$$

where Φ_B is the total volume fraction of B and Φ_{B1} is the volume fraction of non-hydrogen bonded.

3.4. The equilibrium constants of inter-association

Inter-association describes the hydrogen bonding association between two different functional groups as shown in Eq. (7)



where A and C represent the carbonyl group of PVP and the Mannich based bridge of PBZZ, respectively.

In this system, two different types hydrogen bonding are expected to be formed. One is from the hydroxyl group of

PBZZ and carbonyl group of PVP, and the other one is from different segments of the PBZZ (the hydroxyl group and the Mannich-based bridge both of PBZZ).

3.4.1. The inter-association of different molecules

Using a constant dilute concentration (0.02 M) of IPP in CHEX, the fraction of free monomer can be assumed as unity. When the EPr is added, the presence of the carbonyl group of EPr is able to form hydrogen bond with the OH group of IPP. Fig. 3(b) shows that the intensity (fraction) of the IPP hydroxyl at 3620 cm^{-1} decreases drastically with the increase in the EPr content while the hydrogen bonded hydroxyl shifts to low frequency with increasing EPr content, indicating that more fraction of hydrogen bonding is formed. Based on Eq. (8) [1,14,15], those results are summarized in Table 3, and $K_A = 594 \text{ L mol}^{-1}$ is obtained. The mole volume of PBZZ is $129 \text{ cm}^3 \text{ mol}^{-1}$ at room temperature, and $K_A^{\text{Std}} = 4606$ is calculated and is also listed in Table 3.

$$K_A = \frac{1 - f_m^{\text{OH}}}{f_m^{\text{OH}}(C_A - (1 - f_m^{\text{OH}})C_B)} \quad (8)$$

where C_A and C_B denote concentrations of IPP and EPr in L mol^{-1} , respectively.

3.4.2. The inter-association of different segments

By using IPP and DMA as model compounds to investigate the inter-association of different segments, their changes of interaction in distinct molar concentrations are plotted in Fig. 3(c). Because the concentration of the IPP is diluted, the intensity (fraction) of free hydroxyl group of IPP at 3620 cm^{-1} decreases gradually with increasing DMA content. Furthermore, the hydrogen bonding increases insignificantly in spite of increasing the concentration of DMA. This observation implies that the interaction derived from hydroxyl and Mannich based bridge is very weak or insignificant, and the K_C value obtained is very small ($< 10 \text{ L mol}^{-1}$). Since K_A value is significantly greater than K_C , the strong intermolecular interaction due to hydrogen bonding in this system is come from the hydroxyl group of IPP and the carbonyl group of EPr. In summary, the positive T_g composition dependence in PBZZ/PVP blend is due to $K_A > K_B > K_C$.

Table 3

EPr/IPP/CHEX mixture-determination of K_A and K_A^{Std}

C_{EPr} (M)	C_{IPP} (M)	f_m^{OH}	K_A (L mol^{-1})	K_A^{Std} (dimensionless)
0	0.02	–	594 ^a	4606 ^b
0.02	0.02	0.253	583	4508
0.04	0.02	0.076	562	4346
0.08	0.02	0.029	546	4223
0.10	0.02	0.022	540	4175
0.20	0.02	0.011	522	4033

^a Extrapolated to $C_{\text{EPr}} = 0$.

^b Extrapolated to $C_{\text{EPr}} = 0$.

References

- [1] Ishida H. J Appl Polym Sci 1995;58:1751.
- [2] Ishida H, Low HY. Macromolecules 1997;30:1099.
- [3] Ning X, Ishida H. J Polym Sci, Part B: Polym Phys 1994;32:921.
- [4] Schwager F, Eva M, Davis RM. Macromolecules 1997;30:1449.
- [5] Prinos A, Dompros A, Panayiotou C. Polymer 1998;14:3011.
- [6] Kuo SW, Chang FC. Macromolecules 2001;34:5224.
- [7] Wu HD, Chang FC. Polymer 2001;42:555.
- [8] Coleman MM, Painter PC. Prog Polym Sci 1995;20:1.
- [9] Coleman MM, Xu Y, Painter PC. Macromolecules 1994;27:127.
- [10] Kwei TK. J Polym Sci, Poly Lett Ed 1984;22:307.

- [11] Kaczmarek H, Szalla A, Kaminska A. *Polymer* 2001;42:6057.
- [12] Lau C, Mi Y. *Polymer* 2002;43:823.
- [13] Coleman MM, Graf JF, Painter PC. *Specific interactions and the miscibility of polymer blends*. Lancaster, PA: Technomic Publishing; 1991.
- [14] Hu Y, Motzer HR, Etxeberria AM, Fernandez-Berridi MJ, Irin JJ, Painter PC, Coleman MM. *Macromol Chem Phys* 2000;201:705.
- [15] Hu Y, Painter PC, Coleman MM. *Macromol Chem Phys* 2000;201:470.